

Gravitational floating orbits around hairy black holes

Jun Zhang^{1,2,*} and Huan Yang^{2,3,†}

¹Department of Physics and Astronomy, York University, Toronto, Ontario, M3J 1P3, Canada

²Perimeter Institute for Theoretical Physics, Waterloo, Ontario N2L 2Y5, Canada

³University of Guelph, Guelph, Ontario N2L 3G1, Canada

We show that gravitational floating orbits may exist for black holes with rotating hairs. These black hole hairs could originate from the superradiant growth of a light axion field around the rotating black holes. If a test particle rotates around the black hole, its tidal field may resonantly trigger the dynamical transition between a co-rotating state and a dissipative state of the axion cloud. A tidal bulge is generated by the beating of modes, which feeds angular momentum back to the test particle. Following this mechanism, an extreme-mass-ratio-inspiral (EMRI) system, as a source for LISA, may face delayed merger as the EMRI orbit stalls by the tidal response of the cloud, until the cloud being almost fully dissipated. If the cloud dissipation timescale is longer than the average separation between EMRI mergers, it may lead to interesting interaction between multiple EMRI objects at comparable radii. Inclined EMRIs are also expected to migrate towards the black hole equatorial plane due to the tidal coupling and gravitational-wave dissipation.

Introduction. Black Hole (BH) No Hair Theorem states that any stationary black hole in Einstein-Maxwell theory can be characterized by its mass, spin and electric charge, which is possible to be tested with BH spectroscopy in the Advanced LIGO (Laser Interferometric Gravitational-Wave Observatory) era [1–4]. If additional scalar/vector/tensor fields are allowed in the setup, they may grow exponentially according to the BH superradiance [5, 6] and saturate onto stationary or quasi-stationary configurations [7, 8]. In particular, these hair fields (such as the QCD Axion [9], dark photons [10, 11] and string axiverse [12]) around BHs may serve as Dark Matter candidates, and depending on their mass range, they could be dynamically important to the spin evolution of isolated BHs. The rotation of these fields may also generate continuous gravitational waves (GWs) that lie in the detection band of LIGO or LISA (Laser Interferometric Space Antenna) [13–16].

The rotating cloud can carry a significant fraction of energy/angular momentum (AM) of the host BH. Since the BH area generally increases following the superradiant growth of the cloud [8], while interacting with an external agent, the cloud AM would not be entirely re-absorbed by the host BH (e.g., through the tidally-induced cloud depletion discussed in [17]), or its horizon area would decrease. As a result, the external agent must acquire part of the cloud energy/AM during the interaction process. This AM transfer may give rise to *gravitational floating orbits* of a test particle, in which case the GW damping of the orbital energy and AM is balanced by the gravitational interaction with the cloud. Such orbits are first conjectured in [18], based on the observation that the horizon energy/AM flux generated by a test particle orbiting around a rotating BH could be negative due to the superradiance effect. However, for Kerr BHs the energy/AM gain from horizon is universally weaker than the loss due the GW radiation at infinity, which means that there is no gravitational float-

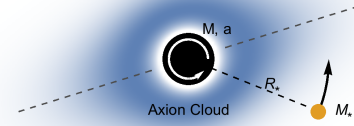


FIG. 1: A host BH of mass M and dimensionless spin a dressed with an axion cloud and accompanied by a star of mass M_* at R_* . The axion cloud develops by superradiance, and is quasi-stationary without the companion star. Through the tidal interaction with the star, a bulge of the cloud develops, which *leads* the motion of the star. In return, the star extracts AM from the BH and the cloud, which could compensate the AM loss of the orbit due to GW radiation. In this case, the star would float at this orbit until the whole cloud is almost fully dissipated.

ing orbit in Kerr spacetime. On the other hand, if the particle also couples to a massive scalar field, it has been shown [19] that the scalar wave radiation can balance the GW radiation, and lead to floating orbits given suitable scalar field mass and coupling strength.

In this *Letter* we show that indeed the tidal interaction between a rotating cloud and a test particle could support gravitational floating orbits, without assuming additional axion field-matter interactions. Physically the test particle tidally deforms the cloud, and because of the cloud dissipation, there is a phase difference between the direction of the test particle and the tidal bulge. Unlike the tidal interactions commonly seen in binary stars, the tidal bulge in the cloud actually leads the test particle’s motion, and consequently energy/AM transfers from the cloud to the test particle.

We examine this cloud energy/AM transfer mechanism in the context of EMRIs, which are important sources

for LISA. We find that for a range of EMRI mass ratio and axion mass, the EMRI orbit stalls at finite radius until the axion cloud is depleted. Notice that this process could take longer than the inspiralling time of the EMRI, which implies interesting astrophysical effects. Unless specifically instructed, we set $G = c = \hbar = 1$.

Toy model. Before performing a detailed analysis, we first illustrate the physical mechanism using a two-mode model. Let us consider a BH with mass M and dimensionless spin a , dressed with axion cloud. Like the electron cloud in a hydrogen atom, the axion cloud also possesses a tower of eigenmodes, which can be denoted by $|nlm\rangle$ with $\{n, l, m\}$ being the principal, orbital, and magnetic “quantum number” respectively. In particular, a mode with $m > 0$ is growing if its eigenfrequency $\omega_{nlm} < m\Omega_H$, with Ω_H being the horizon frequency of the BH, and a mode with $m \leq 0$ is always decaying. Our toy model involves a growing mode and a decaying mode, e.g. $|211\rangle$ and $|21-1\rangle$. At linear level, these two modes evolve independently, but could become coupled in the presence of an external tidal field provided by a companion star. As depicted in Fig. 1, the star has a mass M_* , and for simplicity we assume it is co-orbiting with the BH in a quasi-circular orbit of radius R_* on the equator.

In the interaction picture, the wavefunction of the axion cloud is a linear combination of two modes

$$|\psi(t)\rangle = c_g(t)|\psi_g\rangle + c_d(t)|\psi_d\rangle, \quad (1)$$

where c_g and c_d are the time-dependent amplitudes, with subscripts g and d denoting the growing mode and decaying mode respectively. Initially, $|\psi\rangle$ is normalized as $\langle\psi(0)|\mu|\psi(0)\rangle = M_c$, where μ is the mass of the scalar field and M_c is the mass of the cloud. For a fully grown cloud, i.e. the growing mode is at saturation, $M_c \sim \alpha M$ [15] with $\alpha \equiv \mu M$. In the non-relativistic limit, the coefficients $\mathbf{c} \equiv (c_g, c_d)^T$ satisfy the Schrödinger equation $i d\mathbf{c}/dt = \mathbf{H}_I \mathbf{c}$ with

$$\mathbf{H}_I = \begin{pmatrix} 0 & \eta e^{-i(\Delta m\Omega - \Delta\omega)t} \\ \eta e^{+i(\Delta m\Omega - \Delta\omega)t} & -i\Gamma \end{pmatrix}, \quad (2)$$

where $\Delta m \equiv m_g - m_d$, Ω is the orbital frequency of the companion star, $\Delta\omega \equiv \omega_g - \omega_d$ is the energy split of the two modes, and $\Gamma = -\text{Im}[\omega_d]$ is the damping rate of the $|21-1\rangle$ mode. Following [5], we take $\Gamma \simeq \alpha^{10}/6$ for $\alpha \ll 1$. In the Newtonian limit, the energy split is given by $\Delta\omega \simeq a\alpha^5\mu/6$ and the mode coupling (off-diagonal terms) is induced by the quadrupole tidal perturbations, with $\eta = 9\alpha^{-3}qM^2/R_*^3$ and $q \equiv M_*/M$ [17]. We assume that initially the cloud is saturated, purely consisting of the $|211\rangle$ mode, i.e. $c_g(0) = 1$ and $c_d(0) = 0$. By dynamically evolving $c_g(t)$ and $c_d(t)$, we find that the wavefunction oscillates between the modes with Rabi frequency

$$\omega_R = \sqrt{\eta^2 + (\Delta\omega - \Delta m\Omega)^2}/4 \quad (3)$$

due to tidal coupling, and a resonance occurs when the orbital frequency matches the energy split $\Omega \sim \Delta\omega/\Delta m$.

Next we examine the AM of the axion cloud during the resonance. An immediate expectation is that the cloud loses AM to the BH due to the excitation of the decaying mode. In fact, the AM flux at the horizon can be estimated as

$$\left\langle \frac{dL}{dt} \Big|_H \right\rangle = \frac{-2\Gamma}{T} \int_0^T dt m_d c_d^* c_d = -m_d \Gamma \frac{\eta^2}{2\omega_R^2}, \quad (4)$$

where the time average is taken for many Rabi oscillation periods. Notice that as the decaying mode is losing “negative” AM to the BH, the BH AM changes as $\langle dL_{BH}/dt \rangle = -\langle dL/dt \Big|_H \rangle$. On the other hand, the AM of the cloud can be calculated directly using $c_g(t)$ and $c_d(t)$:

$$L_c = m_g c_g^* c_g + m_d c_d^* c_d, \quad (5)$$

which implies an averaging AM change rate $\langle dL_c/dt \rangle = -m_g \Gamma \eta^2 / 2\omega_R^2$ up to the linear order in Γ . As the total AM is conserved, the AM of the companion star changes as

$$\left\langle \frac{dL_*}{dt} \right\rangle = -\left\langle \frac{dL_{BH}}{dt} \right\rangle - \left\langle \frac{dL_c}{dt} \right\rangle = \Delta m \Gamma \frac{\eta^2}{2\omega_R^2}. \quad (6)$$

The AM gained by the companion star also can be computed by considering the back reaction from the deformed cloud to the star. The tidal density deformation, averaged over many Rabi oscillation periods, is

$$\langle \delta\rho \rangle \simeq \frac{\eta}{2\omega_R^2} \sqrt{4\omega_R^2 + \Gamma^2} \cos[\Delta m(\phi - \Omega t) + \delta\phi] \rho_\times, \quad (7)$$

where $\rho_\times = \exp[i\Delta m\phi] \psi_g^* \psi_d$, and $\sin\delta\phi \equiv \Gamma/\sqrt{4\omega_R^2 + \Gamma^2}$. The deformed density induces additional tangential gravitational acceleration for the star

$$\langle \delta a_\phi \rangle \simeq \frac{\eta^2 \Delta m}{2\omega_R^2} \sqrt{4\omega_R^2 + \Gamma^2} \sin[\delta\phi], \quad (8)$$

which is consistent with Eq. (6).

In this case, one may expect that AM loss of the star due to its GW radiation is compensated by that from the cloud. As a result, the orbital decay stalls because of the AM transfer. Using the balance condition, we find that the companion star floats at an orbit frequency $\Omega_F \equiv (1 - \epsilon)\Delta\omega/2$ with

$$\epsilon \simeq \frac{3^{5/3}\sqrt{5}}{8} \alpha^{5/6} \sqrt{M_c/\alpha M}, \quad (9)$$

until the cloud depletes completely.

BH Perturbation. With the main physical mechanism illustrated in the toy model, we now perform a BH perturbation calculation on hairy BH systems to obtain details in the fully relativistic regime. If the axion’s Compton wavelength is much larger than the size of the BH,

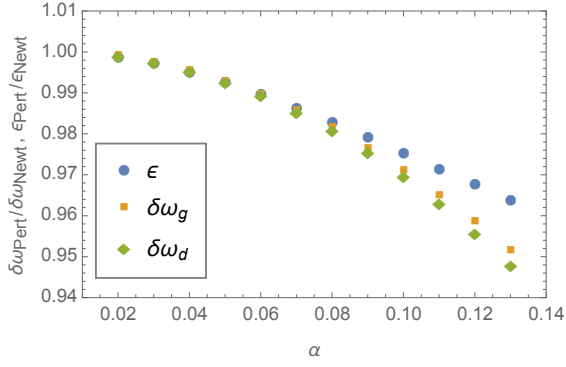


FIG. 2: The ration between quantities calculated using BH perturbation and the Newtonian treatment. $\delta\omega_g$ and $\delta\omega_d$ are the frequency shifts of the $|211\rangle$ and $|21-1\rangle$ modes generated by the tidal field of companion star with $M_* = 10^{-5} M$. ϵ is defined by $\Omega_F \equiv (1 - \epsilon) \Delta\omega/2$ with Ω_F being the floating orbit frequency. We assume that the mass of the axion cloud is αM . In the Newtonian treatment, $\delta\omega_g = \delta\omega_d = -3\alpha^{-3} M_* M / R_*^3$ and ϵ can be estimated by Eq. (9).

although trapped, the support of the axion density profile is away from the BH, which justifies an approximate Newtonian treatment. For more general axion parameters, a BH perturbation analysis is necessary.

The cloud is still assumed to be fully grown to its saturation limit in the absence of a tidal perturber. We approximate the cloud density distribution according to the wave function of the eigenmode [38]. The evolution of a scalar field Ψ with mass parameter μ on a perturbed Kerr background $g = g_{\text{Kerr}} + h$ can be described by

$$\begin{aligned}
(\square_g + \mu^2)\Psi &= 0 \\
&\approx (\square_{\text{Kerr}} + \mu^2)\Psi - \frac{1}{\sqrt{-g_{\text{Kerr}}}} \partial_\mu (h^{\mu\nu} \sqrt{-g_{\text{Kerr}}} \partial_\nu \Psi) \\
&+ \frac{1}{2} g_{\text{Kerr}}^{\mu\nu} (\partial_\mu h^\rho{}_\rho) \partial_\nu \Psi \equiv \left[\square_{\text{Kerr}} + \mu^2 + \frac{1}{\Sigma} \mathcal{H}(h) \right] \Psi,
\end{aligned} \tag{10}$$

where $\Sigma := r^2 + a^2 \cos^2 \theta$, and the operator $\mathcal{H}(\cdot)$ is linear in its argument. We adopt the tidal-deformation metric h from [20], for a slowly rotating black hole with a companion star.

The above wave equation can also be written as $[\square_{\text{Kerr}} + \mu^2] \Psi = S$, with $S \equiv -\frac{1}{\Sigma} \mathcal{H}(h) \Psi$. Formally its solution is

$$\Psi = \int d^4 x' G(x, x') S(x'), \tag{11}$$

with the Green function $G(x, x')$ satisfying

$$[\square_{\text{Kerr}} + \mu^2] G(x, x') = \delta^{(4)}(x - x'). \tag{12}$$

According to the discussion in [21] and taking into account the fact that $\mu \neq 0$, the Green function can be decomposed into two parts in the frequency domain:

$G = G_{\text{dir}} + G_{\text{QNM}}$. The “direct” part G_{dir} generates the propagating waves that travel to spatial infinity or into the BH horizon, with the explicit form unknown. It usually disappears fast for transient sources. The QNM part G_{QNM} generates QNM ringing that we study here. For Kerr BHs it can be expressed as

$$\begin{aligned}
G_{\text{QNM}}(x, x') &= -\frac{2}{\sqrt{r^2 + a^2} \sqrt{r'^2 + a^2}} \\
&\times \text{Re} \left[\sum_m e^{im(\phi - \phi')} \sum_{l, n} Y_{lm}(\theta) Y_{lm}^*(\theta') \right. \\
&\quad \left. \times \mathcal{A}_{nlm} u_{\text{in}}(r) u_{\text{in}}(r') e^{-i\omega_{nlm}(t - t')} \right].
\end{aligned} \tag{13}$$

with $Y_{lm}(\theta)$ being the spheroidal harmonics, ω_{nlm} being the QNM frequency with spherical index l, m and radial overtone n , \mathcal{A}_{nlm} equal to $[2\omega C_{\omega lm}^+ \partial_\omega C_{\omega lm}^-]_{\omega=\omega_{nlm}}^{-1}$ and the scattering coefficient $C_{\omega lm}^\pm$ given in [21]. The wave function u_{in} (nlm sub-indices abbreviated) is just $(r^2 + a^2)^{1/2} R_{\text{in}}$, where R_{in} satisfies the radial Teukolsky equation (c.f. [21]) and is solved in [22] with the bound state boundary condition. Focusing on the QNM Green function, we write the QNM sum as

$$\begin{aligned}
\Psi_{\text{QNM}} &= \sum_{nlm} A_{nlm}(t) e^{-i\omega_{nlm} t} R_{\text{in}}(r) Y_{lm}(\theta) e^{im\phi} \\
&\equiv \sum_{nlm} A_{nlm}(t) e^{-i\omega_{nlm} t} \psi_{nlm} \\
&= \int d^4 x' G_{\text{QNM}}(x, x') S(x').
\end{aligned} \tag{14}$$

As shown in the toy model, mode coupling becomes significant only when the frequency of the perturbation matches the energy split, which allows us to restrict ourselves to a two-mode subspace, as they are the main excitations given a certain external perturbation. The mode equations of motion are [23, 24]

$$\begin{aligned}
\frac{\dot{A}_g}{2\mathcal{A}_g} &\approx A_g \langle \psi_g | \mathcal{H}(h) | \psi_g \rangle + A_d e^{i\Delta\omega t} \langle \psi_g | \mathcal{H}(h) | \psi_d \rangle \\
\frac{\dot{A}_d}{2\mathcal{A}_d} &\approx A_g e^{-i\Delta\omega t} \langle \psi_d | \mathcal{H}(h) | \psi_g \rangle + A_d \langle \psi_d | \mathcal{H}(h) | \psi_d \rangle,
\end{aligned} \tag{15}$$

where the nlm sub-indices are suppressed for abbreviation. The inner product is defined as

$$\langle \psi_{nlm} | \eta \rangle \equiv \int dr \int d\phi \int d\theta \sin \theta R_{\text{in}} Y_{lm}^* e^{-im\phi} \eta, \tag{16}$$

where the integral over r direction has to be regularized to remove apparent singularity of the integrand near the horizon. The regularization can be done using the divergence subtraction method introduced in [25, 26]. According to the discussion in [27–29], $2\mathcal{A}$ can be alternatively evaluated as $-i \langle \psi | \partial_\omega \square | \psi \rangle^{-1}$, with $\tilde{\square}$ being

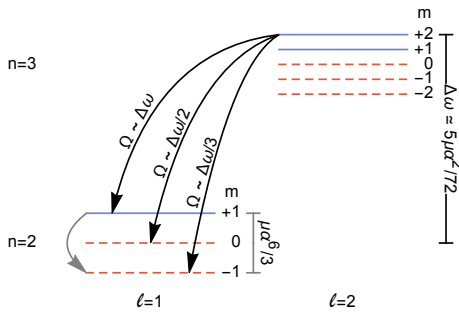


FIG. 3: The eigenfrequencies of modes with $n = 2, l = 1$ and $n = 3, l = 2$. The blue solid lines are the growing modes and the red dashed lines are the decaying modes. Note that when the $|322\rangle$ mode saturates, the $|211\rangle$ mode also becomes a decaying mode. The arrows show the possible resonances associated with a co-rotating companion star.

\square_{Kerr} in frequency space. Notice that the diagonal terms in Eq. (15) generate constant frequency shifts of eigenmodes. The off-diagonal terms generate the transition between modes, and consequently the AM transfer.

Taking $|211\rangle$ and $|21-1\rangle$ as an example, we calculate the frequency shift generated by a companion star and the AM flux at the horizon. We consider the leading quadrupole tidal perturbations and perform the calculation up to the linear order in a . The result and the comparison to that from the Newtonian treatment are shown in Fig. 2. We find that the results start to deviate from their Newtonian counterpart when $\alpha > 0.1$.

Floating Orbits. For astrophysical BHs, the axion cloud is possibly dominated by a saturated mode with $n - 1 = m = l$, where $l = 1, 2, 3, \dots$ depends on the formation time of the BH. In principle, a growing mode could couple to many decaying modes simultaneously. However, an efficient resonance only happens when the orbital frequency Ω is approximately $(\omega_g - \omega_d)/(m_g - m_d)$. This condition has two implications. First, the saturation condition requires that $m_g - m_d > 0$, thus a co-rotating companion star ($\Omega > 0$) can only couple a growing mode to a lower-frequency decaying modes, and vice versa. According to Eq. (6), a companion star only gain positive AM, therefore a floating orbit does not exist for counter-rotating stars ($\Omega < 0$). Secondly, at any orbital frequency, a parent growing mode only efficiently couples to one daughter decaying mode, because the width of the resonance band, characterized by $\epsilon\Delta\omega$ with $\epsilon \sim \alpha^{7/2}$ for the $|322\rangle$ mode for example, is much smaller comparing to the frequency separation between modes which is of the order of $\Delta\omega$. According to Eq. (6), the AM transfer rate depends on the decay rate of the decaying mode, which is proportional to α^{4l_d+5} . Therefore, an efficient transfer is usually provided by the mode with lower l_d . Given the inner product defined in Eq. (16), we find that growing modes always couple to the $|n1-1\rangle$ modes

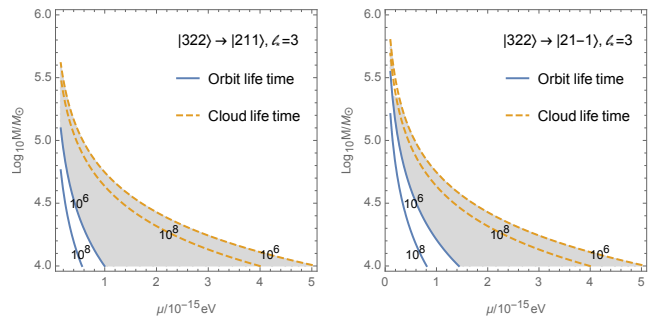


FIG. 4: The parameter space of having a floating orbit caused by the $|322\rangle$ mode coupled to the $|211\rangle$ mode (left panel) and the $|21-1\rangle$ (right panel). We assume the orbit is along the equator of the BH. The blue solid contours show the GW damping time of the floating orbits if there is no axion cloud, and the orange dashed contours show the lifetime of the axion cloud. The shaded region shows the parameters to having a floating orbit with a lifetime greater than 10^6 years. The numbers are in the unit of years.

though a tidal perturbation with $l_* = l_g + 1$.

The eigenfrequencies of the first two growing modes and the relevant daughter modes are shown in Fig. 3. For the $|211\rangle$ mode as a dominant mode, a floating orbit can exist only by its coupling to the $|21-1\rangle$ mode (as shown by the grey arrow in the Fig. 3) [39]. However, the frequency difference between these two modes is $M\Delta\omega \sim \alpha^7/3$, which is so small that the associated floating orbit has a radius of $R_F \sim 3^{2/3}M/\alpha^{14/3}$, far away from the central BH. As a result, the life time of such orbit, even without floating, is usually longer than the lifetime of the cloud. The existence of the axion cloud does not alter the orbit decay significantly, and is of minimal astrophysical relevance.

For the $|322\rangle$ mode, a floating orbit exists by the coupling to the $|211\rangle$ mode or to the $|21-1\rangle$ mode via an octopole tidal perturbation ($l_* = 3$) [39]. For coupling between modes with different n , the floating orbital frequency scales as $M\Omega \sim \alpha^3$. Therefore the orbital radius is comparable to the radius of the axion cloud $R_c \sim M\alpha^{-2}$, namely the companion star is within the axion cloud [40]. Nevertheless, the perturbation method still applies since the mass of the companion star is much smaller than that of the axion cloud. Using the balance condition, we find that, for the coupling to the $|21-1\rangle$ mode, the orbit floats at $\Omega_F = (1 - \epsilon)\Delta\omega/3$ with $\epsilon \simeq 2.6\alpha^{7/2}\sqrt{M_c/\alpha M}$, which is far away from other resonance frequencies, such as, $\Delta\omega$ or $\Delta\omega/2$ for the $|211\rangle$ or $|210\rangle$ mode respectively. In Fig. 4, we present viable physical parameters that allow floating orbits associated with the $|322\rangle$ mode, with the orbit assumed to lie on the equator of the BH. The requirements are two-fold. As the EMRI rate can be estimated as [30]

$$\tau^{-1} \approx 300 \left(\frac{10^6 M_\odot}{M} \right)^{-0.19} \text{Gyr}^{-1}, \quad (17)$$

the orbit lifetime τ (GW damping timescale, Blue Solid lines) of the nearest perturber should be $\mathcal{O}(10^6)$ yrs. On the other hand, at the time of interest, the cloud's dominant mode depends on the BH's formation history and age, as each unstable mode only survives for a finite time due to GW radiation [15, 31]. For the |322> mode, the BH's age should not exceed the mode lifetime (Orange Dashed lines).

Astrophysical Implications. If Axion(s) does exist in the $\mathcal{O}(10^{-15})\text{eV}$ range, some of the EMRIs may stall at the floating orbit instead of inspiralling into the central BH. This could affect merger rates of EMRIs as measured by LISA. However, given the current theoretical uncertainties of merger rates, it is preferable to look for other phenomena associated with this mechanism. For example, if the injected EMRI orbit is inclined (and co-rotating), the GW radiation will damp out the piece of orbital AM on the equatorial plane, leaving the piece orthogonal to the plane supported by the cloud AM transfer. As a result, we may see much more in-plane EMRIs than expected [41]. On the other hand, if an EMRI orbit floats longer than the average time separation between successive EMRIs (τ), it is possible have multiple stellar-mass objects accumulating at comparable radius to the central BH. In addition to the gravitational interaction with the central BH and the cloud, the mutual interaction between these compact objects may lead to very interesting and rich phenomena, such as clustered EMRI mergers, EMRI object ejection, Kozai-Lidov resonance [32–34] and mean-motion resonance [35], etc.

Acknowledgements- We thank Sam Dolan and Horng Sheng Chia for inspiring discussions which initiated this work. J.Z. and H.Y. acknowledge support from the Natural Sciences and Engineering Research Council of Canada, and in part by the Perimeter Institute for Theoretical Physics. Research at Perimeter Institute is supported by the Government of Canada through the Department of Innovation, Science and Economic Development Canada, and by the Province of Ontario through the Ministry of Research and Innovation.

* Electronic address: jun34@yorku.ca

† Electronic address: hyang@perimeterinstitute.ca

- [1] E. Berti, A. Sesana, E. Barausse, V. Cardoso, and K. Belczynski, *Physical review letters* **117**, 101102 (2016).
 [2] H. Yang, K. Yagi, J. Blackman, L. Lehner, V. Paschalidis, F. Pretorius, and N. Yunes, *Physical review letters* **118**, 161101 (2017).

- [3] R. Brito, A. Buonanno, and V. Raymond, arXiv preprint arXiv:1805.00293 (2018).
 [4] E. Thrane, P. D. Lasky, and Y. Levin, *Phys. Rev. D* **96**, 102004 (2017), URL <https://link.aps.org/doi/10.1103/PhysRevD.96.102004>.
 [5] S. L. Detweiler, *Phys. Rev.* **D22**, 2323 (1980).
 [6] T. J. Zouros and D. M. Eardley, *Annals of physics* **118**, 139 (1979).
 [7] W. E. East and F. Pretorius, *Physical review letters* **119**, 041101 (2017).
 [8] W. E. East, *Physical Review D* **96**, 024004 (2017).
 [9] S. Weinberg, *Physical Review Letters* **40**, 223 (1978).
 [10] B. Holdom, *Physics Letters B* **166**, 196 (1986).
 [11] M. Cicoli, M. Goodsell, J. Jaeckel, and A. Ringwald, *Journal of High Energy Physics* **2011**, 114 (2011).
 [12] A. Arvanitaki, S. Dimopoulos, S. Dubovsky, N. Kaloper, and J. March-Russell, *Physical Review D* **81**, 123530 (2010).
 [13] A. Arvanitaki, M. Baryakhtar, and X. Huang, *Physical Review D* **91**, 084011 (2015).
 [14] M. Baryakhtar, R. Lasenby, and M. Teo, *Physical Review D* **96**, 035019 (2017).
 [15] R. Brito, S. Ghosh, E. Barausse, E. Berti, V. Cardoso, I. Dvorkin, A. Klein, and P. Pani, *Phys. Rev.* **D96**, 064050 (2017), 1706.06311.
 [16] R. Brito, S. Ghosh, E. Barausse, E. Berti, V. Cardoso, I. Dvorkin, A. Klein, and P. Pani, *Physical review letters* **119**, 131101 (2017).
 [17] D. Baumann, H. S. Chia, and R. A. Porto (2018), 1804.03208.
 [18] W. H. Press and S. A. Teukolsky, *Nature* **238**, 211 (1972).
 [19] V. Cardoso, S. Chakrabarti, P. Pani, E. Berti, and L. Gualtieri, *Phys. Rev. Lett.* **107**, 241101 (2011), 1109.6021.
 [20] E. Poisson, *Phys. Rev.* **D91**, 044004 (2015), 1411.4711.
 [21] H. Yang, F. Zhang, A. Zimmerman, and Y. Chen, *Physical review D* **89**, 064014 (2014).
 [22] S. R. Dolan, *Phys. Rev.* **D76**, 084001 (2007), 0705.2880.
 [23] H. Yang, A. Zimmerman, and L. Lehner, *Physical review letters* **114**, 081101 (2015).
 [24] H. Yang, F. Zhang, S. R. Green, and L. Lehner, *Physical Review D* **91**, 084007 (2015).
 [25] E. W. Leaver, *Phys. Rev.* **D34**, 384 (1986).
 [26] S. L. Detweiler and E. Szedenits, *Astrophys. J.* **231**, 211 (1979).
 [27] A. Zimmerman, H. Yang, Z. Mark, Y. Chen, and L. Lehner, in *Gravitational Wave Astrophysics* (Springer, 2015), pp. 217–223.
 [28] Z. Mark, H. Yang, A. Zimmerman, and Y. Chen, *Physical Review D* **91**, 044025 (2015).
 [29] H. Yang and F. Zhang, *The Astrophysical Journal* **817**, 183 (2016).
 [30] J. R. Gair, S. Babak, A. Sesana, P. Amaro-Seoane, E. Barausse, C. P. Berry, E. Berti, and C. Sopuerta, in *Journal of Physics: Conference Series* (IOP Publishing, 2017), vol. 840, p. 012021.
 [31] H. Yoshino and H. Kodama, *PTEP* **2014**, 043E02 (2014), 1312.2326.
 [32] Y. Kozai, *The Astronomical Journal* **67**, 591 (1962).
 [33] M. Lidov, *Planetary and Space Science* **9**, 719 (1962).
 [34] H. Yang and M. Casals, *Physical Review D* **96**, 083015 (2017).
 [35] J. J. Souchay and R. Dvorak, *Dynamics of small solar system bodies and exoplanets*, vol. 790 (Springer, 2010).

- [36] C. Herdeiro and E. Radu, *Classical and Quantum Gravity* **32**, 144001 (2015).
- [37] N. Yunes, B. Kocsis, A. Loeb, and Z. Haiman, *Physical review letters* **107**, 171103 (2011).
- [38] The exact solution can be found in [36], and the numerical solution is presented in [8]. Eigenmode is a good approximation as the cloud energy is generally small comparing to the BH mass.
- [39] If the orbit is not along the equator, the companion star could also extract AM through the coupling between the $|211\rangle$ and $|210\rangle$ modes. However, AM gained by the star is always orthogonal to the BH equator, while star's AM on the equator plane decays by GW radiation. In this case, the incline angle of the orbit (and hence the coupling) will vanish in a GW damping timescale. Therefore, the coupling does not alter the orbit decay significantly. There is a similar situation for the coupling between $|322\rangle$ and $|210\rangle$ through the octopole tidal perturbations.
- [40] The timescale for the cloud to be absorbed by the stellar-mass BH is much longer than the cloud lifetime.
- [41] If there is a gaseous disk around the central BH, the disk migration may also generate similar effect [37].